Wind and Structures, *Vol. 32, No. 1 (2021) 71-80*
DOI: https://doi.org/10.12989/was.2021.32.1.71

Wind vibration control of stay cables using an evolutionary algorithm

Tim Chen[1], Yu-Ching Huang*[2,3], Zhao-Wang Xu[2] and J.C.Y. Chen[4]

[1]Faculty of Information Technology, Ton Duc Thang University, Ho Chi Minh City, Vietnam
[2]Department of Earth Science, National Taiwan Normal University, Taipei, China
[3]Center of Natural Science, Kaohsiung Municipal Fushan Junior High School, Kaohsiung, China
[4]Faculty of Information Technology, University of California, Irvine, U.S.A.

(*Received December 4, 2019, Revised January 11, 2021, Accepted January 22, 2021*)

Abstract. In steel cable bridges, the use of magnetorheological (MR) dampers between butt cables is constantly increasing to dampen vibrations caused by rain and wind. The biggest problem in the actual applications of those devices is to launch a kind of appropriate algorithm that can effectively and efficiently suppress the perturbation of the tie through basic calculations and optimal solutions. This article discusses the optimal evolutionary design based on a linear and quadratic regulator (hereafter LQR) to lessen the perturbation of the bridges with cables. The control numerical algorithms are expected to effectively and efficiently decrease the possible risks of the structural response in amplification owing to the feedback force in the direction of the MR attenuator. In addition, these numerical algorithms approximate those optimal linear quadratic regulator control forces through the corresponding damping and stiffness, which significantly lessens the work of calculating the significant and optimal control forces. Therefore, it has been shown that it plays an important and significant role in the practical application design of semiactive MR control power systems. In the present proposed novel evolutionary parallel distributed compensator scheme, the vibrational control problem with a simulated demonstration is used to evaluate the numerical algorithmic performance and effectiveness. The results show that these semiactive MR control numerical algorithms which are present proposed in the present paper has better performance than the optimal and the passive control, which is almost reaching the levels of linear quadratic regulator controls with minimal feedback requirements.

Keywords: semiactive intelligent control; magnetorheological; optimal equivalent controller design; vibrational control and numerical algorithmic design

1. Introduction

As the main load-bearing part of the quadruple bridge, the fixed cable will be affected by perturbation in rain and wind due to its low damping characteristics and kind of low inherent mass density, so the risk is higher when the life and property is exposed in treachery environments (Qissab and Salman 2018, Orod *et al*. 2016, Akgöz and Civalek 2013, Djebien *et al*. 2018, Goksu *et al*. 2019, Muthuraj *et al*. 2017). Thus, it was very important to launch a technology that can effectively and efficiently control and suppress the perturbation of the cables caused by rain and wind. Usually, different attenuation units are mounted in the bridge cables, and the focus is on improving the nonlinear dynamic behaviors and reducing the structural response. The so-called viscous typed tuned mass damper and its advanced application and advantages on resonance are used for a number of examples. As the attenuation unit, the semi active MR attenuator has good controllability, fast response, low power consumption and excellent adaptability, so it has obvious constructive advantages. Therefore, it has proven to be relatively appropriate for controlling the perturbation among the choices of traditional control laws. Johnson *et al*. (2019) conducted a study on the topic of the semiactive control power system, and the results showed that the semi active MR control power system can achieve a higher modal attenuation ratio than the best passive viscose. According to the inverse space theory, the previous study in Duan *et al*. (2018) indicates a state feedback transition numerical algorithm that only requires feedback in the acceleration data to attenuate the perturbation of cables which are provided with MR attenuators. Weber *et al*. (2017) used passive control numerical algorithms highlighting the effectiveness of vibrational control of magnetic control resonance attenuators with stay cables. The results describe that the optimization damping-reduced force is inversely proportional to the mode sequence, indicating that a higher damping-reduced force is required to handle low-frequency vibrations. Weber *et al*. (2018) also announced the merits of the linear and quadratic Gaussian algorithm (LQG) model-based approaches on the energy diffusion cases, it is observed that the MR attenuator can be denoted such like a viscous attenuation control, and can feasibly and efficiently decrease the force and vibrational ranges of any frequency. The previous study in Zhou *et al*. (2018) launched a semiactive control strategy according to an approximated friction with homogeneous numerical algorithm to dampen the 3D perturbation of the cable using a separate MR damper. The previous study in Christenson *et al*. (2016) then put forward a control numerical algorithm according to the numerical feedback of the relative moving

*Corresponding author, Professor
E-mail: jc343965@gmail.com

http://www.techno-press.com/journals/was&subpage=7
ISSN: 1226-6116 (Print), 1598-6225 (Online)

from its place or position and the modification of the vibrational absorber to deal with the perturbations, in which the significant reduction in the vibrational response can reach 50%. According to the control-centric model of Johnson (2018), Li *et al*. (2018) took advantage of LQG active control and limited Hrovat semiactive control strategies to separate cable vibrational attenuation through MR attenuators. By applying the principle of energy equivalence to the vibrational control of cables equipped with magnetic control resonance attenuators, Weber and Boston (2015) then proposed an optimal linear passive friction attenuation theory. Zhao and Zhu (2016) put forward the Hamilton system with the best semiactive stochastic control numerical algorithm to lessen the perturbation of multimode cables using magnetic control resonance attenuators. Caterino (2016) conducted an experiment of simulating table on a 0.05 scale miniature to study the damping effect of the semiactive MR attenuator on vibration subjected to a wind perturbation. Chen *et al*. (2018) put forward a self-test magnetic control imaging cushion structural mechanism to demonstrate and decrease the perturbation of the cable. Furthermore, Park *et al*. (2019), Ni *et al*. (2018), and Ok *et al*. (2019) took advantage of neural intelligent network design and particular fuzzy rule based system with feedback controlled technology to deal with the perturbation in the handlebar cable. According to the control force characteristics of the linear and quadratic regulator clamp, Weber and Distl (2012) derived the best control device to lessen the perturbation during the semiactive attenuation and negative stiffness of the multimode cable. This near-optimal control solution does not require the health assessment of the observer model, so it can be easily and inexpensively implemented using cables.

However, owing to the complexity of the semiactive MR controlled design, the real-time electronic intelligent performance and theory are difficult to prove its rationality. Therefore, a reliable semiactive MR control power system is rarely exploited to attenuate the perturbation of the stay cable. In 2001, the famous Lake Bridge introduced the first MR attenuator on the control line to control wind perturbation by Xu *et al*. (2018). Weber and Distl (2012) took advantage of a semiactive MR control power system to control the perturbation of the bridge where the system took advantage of an attenuation control monitoring numerical algorithm to control the effects of temperature.

Obviously, the semiactive MR control power system in the actual structure is not widely exploited for vibrational control of the cable. The possible reasons could be lacking of proper stability analysis and solvable algorithms, simplified demonstration with good simulation of vibrational reduction. Afterwards, this article provides an optimal and kind of equivalent control numerical algorithm, which is taking account into the directions of the parallel distributed compensation scheme. The present proposed biological numerical algorithm effectively and efficiently lessens the dynamic response of these cables, while greatly simplifying the calculation of the practical engineering applications.

The structure of this article is as the following. First, design and review a new evolutionary MR shock absorber by testing its mechanical properties. Followed by the best description of the corresponding control numerical algorithm. In addition, by using a controlled MR attenuator to simulate a wind-induced residential cable, the simulated performance of the present developed evolutionary numerical algorithm is proved. Then we compared the results with the best passive control and linear and quadratic regulator control and drawled a conclusion.

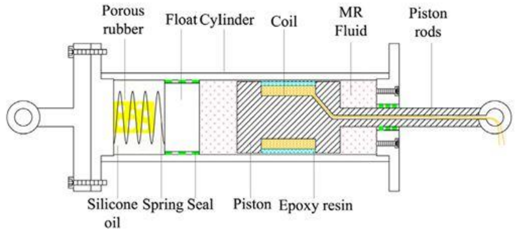

Fig. 1 The mechanism of damper structure with float cylinder and MR fluid

2. Structure problems and motion systems

In this article, our research team designed and put forward an MR attenuator. This could be novel and kind via a spring-loaded float cylinder in device. The advantages of the cushion are large working strokes and and kind of less installation cost and size, which could feasibly and efficiently avoid the trouble with its air gap particularly in the period of installation. The device uses the knowhow of insulation volume solving couple volume compensation troubles like the profile as indicated in Figure 1. The floating point separates the chamber volume completed by adjusting the volume. The magnetic control circuit of the magnetic control imaging damper is mainly composed of an outer cylinder, a piston, a magnetic control imaging fluid and a cushion port. The winding coil is wound in the middle of the piston, and the outer cylinder is a magnetic control cylinder head that leads to the closed magnetic control circuit. These outer cylinders and the pistons are kind of part of the magnetic control circuit and the major brace in these entire structures. These dampers are filled with an anti-settling magnetic control resonance fluid put forward by our research team. Therefore, the advantages of these shock absorber distributions are improved. These pistons and piston rods are DT4 electric irons with high permeability and low residual. The other parts in the center of these piston are copper wires with a diameter of 1 mm, and the maximum current is 2A. The magnetic control circuit of the single rod MRI attenuator have been optimized in the study, and its design parameters are indicated as seen in Table 1.

In order to derive the engineering performance of the vibrational absorber, the single rod magnetic control absorber was constructed and the test parameters are shown in Fig. 2. Separated disturbing frequency f and amplitude A are applied in the damper in the study to check its mechanical performance under separated currents. In the

Table 1 The numerical experimental data in construction of the design

Content	Parameter	Content	Parameter
Cylinder outer diameter	62 mm	Excavated width	50 mm
Cylinder Inner diameter	52 mm	number of field turns	300
Piston diameter	50 mm	Total length of piston	207 mm
Piston rod diameter	14 mm	Working stroke	±50 mm
Effective gap length	50 mm	Spring stiffness	236 N/mm
Damping gap width	1.0 mm	Diameter of threading hole	4 mm
Excavated depth	14 mm	Range of working current	0e1.5 A

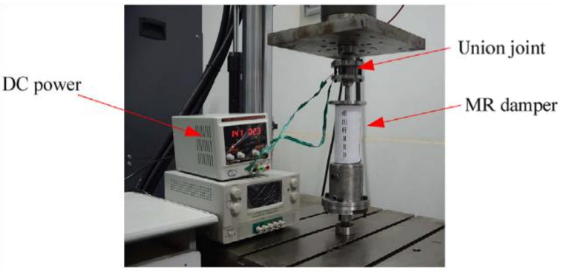

Fig. 2 The equipment for the absober efficiency test

study, we obtained one thousand Hz sampling rate compensation and corresponding attenuation power under each test condition. Then, the corresponding speed in the study could be given through a separate calculus.

In order to eliminate the abnormal data caused by the instability of the numerical experimental equipment, the mechanical performance of the damper was evaluated by centering the data loop on the outside of the first and last two turns. Fig. 3 shows the different currents of the transmission power profile and - speed profile as 7.5 mm respectively correspond to the excitation amplitude and frequency of 1 Hz.

Fig. 3 demonstrates that although no input applied to the design, the transmission hysteresis curve is essentially an ellipse, showing the tuned mass damper merits in the design. As the current increases, the slope fi of the maximum power output and the maximum yield strength of the absorber will also increase significantly. It is a progressive rectangular image, and it presents a force-displacement curve. The power transfer curve gradually fills up as the current gradually increases. This indicates a significant increase in the slope acoustic power loss capacity as the shutter current increases. Again, it is shown from Fig. 3 that the power speed curve with increasing current exhibits obvious hysteresis characteristics at low speed.

Because of magnetic control saturation of the damper force can reach 1.65 kN, the damper force can only reach 0.79 kN, which indicates that the MR damper can be exploited in MR semiactive control power systems owing to its continuously adjustable damping-reduced force. Owing to the current oscillation and low amplitude of the cable, the principle exploited in the MR design is that under normal conditions (the perturbation is not serious), the MR attenuator has no power supply. When the actual oscillation amplitude of the cable have reached a certain value, and the numerical algorithm will control the plant, and it changes in real time will become the input of the attenuator MR. Therefore, the ratio of maximum power and maximum

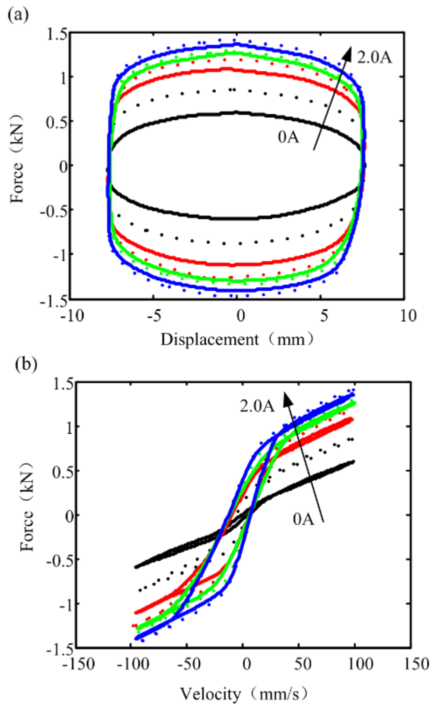

Fig. 3 The relationship of the practical numerical experiments for (a) force (kN)-displacement (mm) and (b) force (kN)-velocity (mm/s)

power response of zero power is not great, because it is the official technical benefits of science fiction long-term use of impact MR.

3. Intelligent control power system

The point of this section is the one-dimensional perturbation of the stay cable, in which a magnetic control resonance damper is equipped near the cable support point, as indicated in Fig. 4. These vibrational responses selected in the plant evaluates the control power of the cable with the MR control power system and design model. The cable motion equation can be expressed by a magnetic control resonance attenuator

$$\dot{x}(t) = f(x, u)$$

where state vector $x(t)$, unit input vector $u(t)$ and unit vector-valued function f all satisfies those assumptions of general continuity and boundedness referred to Steinberg and Kadushin (1973).

In order to facilitate the introduction of the structure of the control power system, the evolutionary intelligent numerical algorithm for the controlled system is divided into two parts. The Takagi-Sugeno type fuzzy numerical model is created for the system and parallel distributed compensator (PDC) techniques for designing fuzzy system controller, and a stability criterion is taken into account to determine whether the fuzzy feedback controlled system $F(C;0)$ is stable.

the kind of closed-loop state feedback fuzzy controlled system $F(C;0)$:

$$\dot{x}(t) = \frac{\sum_{i=1}^{r}\sum_{j=1}^{r} w_i(x(t))w_j(x(t))\{A_i - B_iK_j\}x(t)}{\sum_{i=1}^{r}\sum_{j=1}^{r} w_i(x(t))w_j(x(t))} \tag{1}$$

Which be rewritten as

$$\dot{x}(t) = \frac{1}{W}\left[\sum_{i=1}^{r} w_i(x(t))w_i(x(t))\{A_i - B_iK_i\}x(t) + 2\sum_{i<j}^{r} w_i(x(t))w_j(x(t))G_{ij}x(t)\right] \tag{2}$$

For the clarification of the Lyapunov theory in stability analysis, some principles are well-known that $Q = P^{-1}$ (common positive definite matrix, referred in Wang *et al.*, (1996)) and we therefore obtain $W_i = K_iQ$, so that for $Q > 0$ we have $K_i = W_iQ^{-1}$. Hence, according to the Lyapunov linear matrix inequality (LMI) approach, Lemma 2 could be given to ensure the asymptotic stability of $F(C;\ 0)$.

Lemma 2 (Wang and Tanaka, 1996) The kind of closed-loop fuzzy feedback controlled system is asymptotically and significantly stable in the large via parallel distributed compensator (PDC) if there exist the following linear matrix inequality (LMI) sufficient conditions with appropriate operations:

$$QA_i^T + A_iQ - B_iW_i - W_i^TB_i^T < 0$$

Next, according to Lemma 2, we synthesized the brightness variables to stabilize the system. However, not all fuzzy system controls can meet the stability criteria and be exploited to applied in practical controlled systems. This means that there may a fuzzy stability control fails to control the real nonlinear plant. Therefore, the kind of closed-loop control systems are divided into two types for our design.

Type 1: If the common definite matrix in Lyapunov LMI could be feasibly determined satisfying the conditional stability of Lemma 2, then the PDC fuzzy system controller can be successfully exploited to stabilize the system.

Type 2: If there is no normal positive definite matrix or the stability conditions of Lemma 2 are not satisfied, implying the controller cannot be utilized to make systems stabilized, then an auxiliary tool of the fuzzy system controller will be put forward and deployed to stabilize the system asymptotically.

Therefore, a polished attention will be described in the following for the stability analysis of the fuzzy controlled system $F_2(C;\ 0)$.

The T-S fuzzy numerical model of the controlled system $N_R(0;\ 0)$ is in the study established subsequently for the prepare of a fuzzy system controller acquired via the PDC scheme.

The ith rule kind of the fuzzy numerical model unit $F_R(0;\ 0)$ is demonstrated as the following:

Fuzzy ruled model design: The ith rule of the fuzzy system controller is given as

Control Rule i:

IF $x_{R1}(t)$ is $M_{i1}^R(\alpha_m, \beta_m)$ and … and $x_{Rk}(t)$ is unit $M_{ik}^R(\alpha_m, \beta_m)$

THEN $u_R(t) = -K_i(\alpha_m, \beta_m)x_R(t)$

Thus, the overall fuzzy system controller is

$$u_R(t) = -\frac{\sum_{i=1}^{r} w_i(x_R(t), \alpha_m, \beta_m)K_i(\alpha_m, \beta_m)x_R(t)}{\sum_{i=1}^{r} w_i(x_R(t), \alpha_m, \beta_m)}$$

The derive the kind of closed-loop fuzzy control system unit $F_R(C;0)$ as the following

$$\dot{x}_R(t) = \frac{\sum_{i=1}^{r}\sum_{j=1}^{r} w_i(x_R(t), \alpha_m, \beta_m)w_j(x_R(t), \alpha_m, \beta_m)\{A_i(\alpha_m, \beta_m) - B_i(\alpha_m, \beta_m)K_j(\alpha_m, \beta_m)\}x_R(t)}{\sum_{i=1}^{r}\sum_{j=1}^{r} w_i(x_R(t), \alpha_m, \beta_m)w_j(x_R(t), \alpha_m, \beta_m)} \tag{3}$$

From the above derived control laws, it can be concluded that, if the rasterization having a sufficiently high frequency of the right member function is selected, the frequency for the stability could be guaranteed for the kind of closed-loop control system and a real nonlinear system made as close as possible (Zames Shneydor 1976, 1977, Wang and Abed 1995). By assigning it to the weak kind of closed-loop control system, the stability of the kind of closed-loop control system can be strictly predicted.

4. LMI stability design and evolutionary PDC fuzzy numerical algorithm

For now, we will focus on the stability of the kind of closed-loop fuzzy control system $F_R(C;\ 0)$ instead of discussing the stability of the original kind of closed-loop control system $N(C;\ d)$. Hence, the stability criterion of $F_R(C;\ 0)$ is presented as the following.

Theorem 1 The kind of closed-loop fuzzy feedback controlled system is asymptotically and significantly stable in the large via the evolutionary numerical algorithmic PDC design if there exist a $Q > 0$ and $W_i(\alpha_m, \beta_m)$, $i = 1, 2, \ldots, r$ such that these LMI Lyapunov sufficient conditions hold below

$$\begin{aligned}
&QA_i^T(\alpha_m, \beta_m) + A_i(\alpha_m, \beta_m)Q - B_i(\alpha_m, \beta_m)W_i(\alpha_m, \beta_m) \\
&-W_i^T(\alpha_m, \beta_m)B_i^T(\alpha_m, \beta_m) < 0 \\
&QA_i^T(\alpha_m, \beta_m) + A_i(\alpha_m, \beta_m)Q + QA_j^T(\alpha_m, \beta_m) + A_j(\alpha_m, \beta_m)Q \\
&- B_i(\alpha_m, \beta_m)W_j(\alpha_m, \beta_m) \\
&-W_j^T(\alpha_m, \beta_m)B_i^T(\alpha_m, \beta_m) - B_j(\alpha_m, \beta_m)W_i(\alpha_m, \beta_m) \\
&-W_i^T(\alpha_m, \beta_m)B_j^T(\alpha_m, \beta_m) < 0
\end{aligned} \tag{4}$$

where $W_i(\alpha_m, \beta_m) = K_i Q$, $W_j(\alpha_m, \beta_m) = K_j Q$.
The proof of the above fuzzy ruled based feedback theorem can be similarly obtained by the similar derivation like Wang and Tanaka (1996) but more advanced process cause the consideration of dithered injection with systematic matrix being replaced by $A_i(\alpha_m, \beta_m)$, $A_j(\alpha_m, \beta_m)$, $W_i(\alpha_m, \beta_m)$ and $W_j(\alpha_m, \beta_m)$, respectively. This proof is similar to Wang and Tankaka (1996) but lengthier, therefore it is not repeated here.

The whole design process can be summarized as the following numerical algorithm.

Question: How to synthesize the attenuator in the system and find the appropriate injected dithered signal to stabilize these closed loop systems?

According to the following steps, the parameter result is correctly selected to transfer the artificial intelligenceagent to the solution area. This means improving the accuracy to find a solution that is close to the best and reducing the possibility of falling to a local optimum. The medium chosen in our numerical experiment is air, because air is the kind of original medium in the study in the natural and real environment in which the bats live. This is a brief description of EBA activities:

Step 1: Build a system of fuzzy numerical model TS.

Step 2: When designing a fuzzy system controller, the PDC scheme will be considered to design for the fuzzy feedback controlled systems. Then adjust the feedback gain and use Lemma 2 to verify the stability of the kind of closed-loop control system $F(C;\ 0)$.

Step 3: If the stability condition of Lemma 2 cannot be satisfied by adjusting the feedback gain, a dither, as an following auxiliary of the fuzzy system controller, is injected into $N(0;\ 0)$.

Step 4: Apply the method to build the corresponding model.

Step 5: Reconstruct the T-S fuzzy numerical model of $N_R(0;\ 0)$ and use the PDC scheme to deduce the fuzzy system controller.

Step 6: Derive the kind of closed-loop fuzzy control system by substituting the fuzzy system controllerinto the fuzzy numerical model. Furthermore, adjust the parameters (α_m, β_m) of the dither to satisfy the stability criterion of Theorem 1 (Mossaheb, 1983).

Step 7: Disperse the artificial intelligencesubstance in a solution state to make it have random coordinates.

Step 8: Generate a random number, and then check whether it was greater than the fixed pulse discharge rate. Upon the result is kind of positive, then the man-made medium is moved through a random roaming process. $x_i^t = x_i^{t-1} + D$ in which x_i^t denotes the coordinate of the unit ith artificial intelligenceagent at the tth iteration, x_i^{t-1} denotes the coordinate of the unit ith artificial intelligenceagent at the last iteration, and unit D is these moving distances that the artificial intelligenceagent goes in the iterations.

$D = \gamma \cdot \Delta T$ in which γ is kind of a constant corresponding to the kind of medium chosen in the numerical experiment, and $\Delta T \in [-1,1]$ is kind of a random number. $\gamma = 0.17$ is exploited in our numerical experiment because these chosen mediums are air.

[illegible], $\beta \in [0,1]$ in which β is kind of a random number; x_{best} denotes the coordinate of the kind of near best solution found so far in the present study throughout all artificial intelligenceagents; and $x_i^{t_R}$ represents the kind of new coordinates of the artificial intelligenceagent after the operation of the kind of random walk process.

Step 9: Use the user-defined training function to calculate the matching degree of the device and update it to the closest best storage solution.

Step 10: Check the shutdown status to decide in the present study whether to return to step 8 or close the program and submit a solution that is close to the best.

The training function exploited in the evaluation process in the present study is a set of user-defined criteria. That is, the learning function is kind of a mathematical representation of these solution fields, and the user wants to solve the problem or find the best solution for it. Therefore, in this article, the design of the motion function is to find a positively defined symmetric matrix and the output force of these controllers.

5. Numerical experiment and simulation result

The high-rise buildings with ATMD could be lumped in the motion equation type with an ATMD equipped on the top floor as

$$\mathbf{M}\ddot{\mathbf{x}} + \mathbf{C}\dot{\mathbf{x}} + \mathbf{K}\mathbf{x} + \mathbf{H}\mathrm{u} = \eta\mathbf{W}$$

in which moving from its place or position vector $\mathbf{x} = [x_1, x_2, ..., x_{76}, x_m]'$ between the ith floor and xm of the inertial damper mass with respect to these top floors denotes the vector transpose in M, C, and K (77 x 77) matrices to represent mass, stiffness and damping, where u, H, η and W denote control force, control influence, excitation influence and wind excitation input.

The resulting state equation is given by

$$\dot{\mathbf{x}} = \mathbf{A}\mathbf{x} + \mathbf{B}\mathrm{u} + \mathbf{E}\mathbf{W}$$

The dimensionless version of this performance standard consists of

$$J_1 = \max\left\{ \frac{\sigma_{\ddot{x}1}}{\sigma_{\ddot{x}75o}}, \frac{\sigma_{\ddot{x}30}}{\sigma_{\ddot{x}75o}}, \frac{\sigma_{\ddot{x}50}}{\sigma_{\ddot{x}75o}}, \frac{\sigma_{\ddot{x}55}}{\sigma_{\ddot{x}75o}}, \frac{\sigma_{\ddot{x}60}}{\sigma_{\ddot{x}75o}}, \frac{\sigma_{\ddot{x}65}}{\sigma_{\ddot{x}75o}}, \frac{\sigma_{\ddot{x}70}}{\sigma_{\ddot{x}75o}}, \frac{\sigma_{\ddot{x}75}}{\sigma_{\ddot{x}75o}} \right\}$$

where rms acceleration $\sigma_{\ddot{x}i}$ with the ith floor, rms acceleration $\sigma_{\ddot{x}75o} =$ 9.914 with up to 75th floor are well-known with performance criterion J_1. The standardized version is in Eqs. (5)-(6).

$$J_3 = \max\left\{ \frac{\sigma_{x1}}{\sigma_{x76o}}, \frac{\sigma_{x30}}{\sigma_{x76o}}, \frac{\sigma_{x50}}{\sigma_{x76o}}, \frac{\sigma_{x55}}{\sigma_{x76o}}, \frac{\sigma_{x60}}{\sigma_{x76o}}, \frac{\sigma_{x65}}{\sigma_{x76o}}, \frac{\sigma_{x70}}{\sigma_{x76o}}, \frac{\sigma_{x75}}{\sigma_{x76o}}, \frac{\sigma_{x76}}{\sigma_{x76o}} \right\} \quad (5)$$

$$J_4 = \frac{1}{7}\sum_i[(\sigma_{xio} - \sigma_{xi})/\sigma_{xio}] \quad (6)$$

where σ_{xi} and σ_{xio} represent the actual ground moving from its place or position with and without input respectively, and unit σ_{x76o} = 10.040 cm is saying the rms moving from its place or position of the uncontrolled building.

Each present proposed control structure must comply with the given capacity limit actuator, respectively, given by unit $\sigma_u \le 100\,\text{kN}$ and unit $\sigma_{xm} \le 25\,\text{cm}$ with rms control σ_u and rms actuator σ_{xm}, respectively. With respect to the above restrictions, the requirements of the present proposed control design must be evaluated according to the following dimensionless criteria:

$$J_5 = \sigma_{xm}/\sigma_{x76o}$$

$$J_6 = \sigma_{\dot{x}m}/\sigma_{\dot{x}76o}$$

in which unit $\sigma_{\dot{x}m}$ is saying the rms actuator velocity and the performance criteria correspond to the physical size (i.e., stroke) and control power (i.e., actuator velocity) of the actuator calculated without control, including $\sigma_{\dot{x}76o}$ = 9.328.

A numerical simulation model (integration) for the kind of on-line implementation of the present proposed control design in the present study should be conducted in order to evaluate the performance in terms of the following non-dimensionalized criteria

$$J_7 = \max\left\{\frac{\ddot{x}_{p1}}{\ddot{x}_{p75o}}, \frac{\ddot{x}_{p30}}{\ddot{x}_{p75o}}, \frac{\ddot{x}_{p50}}{\ddot{x}_{p75o}}, \frac{\ddot{x}_{p55}}{\ddot{x}_{p75o}}, \frac{\ddot{x}_{p60}}{\ddot{x}_{p75o}}, \frac{\ddot{x}_{p65}}{\ddot{x}_{p75o}}, \frac{\ddot{x}_{p70}}{\ddot{x}_{p75o}}, \frac{\ddot{x}_{p75}}{\ddot{x}_{p75o}}\right\}$$

$$J_8 = \frac{1}{6}\sum_i[(\ddot{x}_{pio} - \ddot{x}_{pi})/\ddot{x}_{pio}]$$

$$J_9 = \max\left\{\frac{x_{p1}}{x_{p76o}}, \frac{x_{p30}}{x_{p76o}}, \frac{x_{p50}}{x_{p76o}}, \frac{x_{p55}}{x_{p76o}}, \frac{x_{p60}}{x_{p76o}}, \frac{x_{p65}}{x_{p76o}}, \frac{x_{p70}}{x_{p76o}}, \frac{x_{p75}}{x_{p76o}}, \frac{x_{p76}}{x_{p76o}}\right\}$$

$$J_{10} = \frac{1}{7}\sum_i[(x_{pio} - x_{pi})/x_{pio}];$$

where peak moving from its place or position $\ddot{x}_{pi}$, x_{pio} without control, for example, x_{p76o} = 26.009 and $\ddot{x}_{p75o}$ = 26.334 are obtained via fuzzy feedback numerical algorithm present proposed in Eq. (3).

The actuator capacity in deterministic response analysis is limited to $\max|u(t)| \le 300\,\text{kN}$ and $\max|x_m(t)| \le$ 75 cm. Additionally, the present proposed control plan should be evaluated according to the following controllability criteria

$$J_{11} = x_{pm}/x_{p76o}$$

$$J_{12} = \dot{x}_{pm}/\dot{x}_{p76o}$$

where actuator peak stroke x_{pm}, actuator peak velocity $\dot{x}_{pm}$ and 76th floor peak velocity $\dot{x}_{p76o}$ calculated 22.622 are with no control force.

During the random wind load, we compare the state of displacement, acceleration and velocity response with the semiactive and uncontrolled 50% relative cable length of Fig. 5. The conclusion drawn from these figures are that the semiactive control numerical algorithm according to the best similar model can effectively and efficiently lessen the vibrational response of the cable by significantly reducing the velocity, displacement and the acceleration response which is compared with the uncontrolled state.

This compares the displacement, speed and acceleration response time history curves of the cable under 50% relative length under passive, semiactive and optimal linear and quadratic regulator control shown in Fig. 6. In terms of damping the perturbation of the cable through the absorber, the control effect of semiactive control is then significantly better than passive fuzzy control. The result is slightly worse than the linear and quadratic regulator control numerical algorithm. In order to more check the vibrational performance of the semiactive control numerical algorithm, we list the maximum standardized values in the displacement, acceleration and velocity within 100-200 seconds. The results show that the apparent control efficiency at the maximum displacement, the speed and the acceleration of the semiactive control cable are lessend by 21.4%, 30.0% and 34.2% which is compared to uncontrolled results, and which is compared to 5.5%, 7.3%, and 11.7, respectively. While Comparing with the uncontrolled results of 12.6%, 18%, 2% and 47.4%, the linear and quadratic regulator control lessens 25.9 percentages (optimal compensation), 43.0 percentages (optimal speed) and 58.3 percentages (optimal acceleration), respectively. This shows that the performance of semiactive control is more dominant than that kind of average intelligent passive fuzzy control and worse than that of linear and quadratic regulator control.

We obtain the typical RMS acceleration, velocity, and moving from its place or position with the best performance of semiactive drives in terms of vibrational reduction. The results show that the performance of the semiactive control power system in reducing the RMS cable response is significantly better compared to the best passive system. For simulation with uncontrolled conditions, the best traditional fuzzy control can lessen displacement, speed and acceleration by 12.87%, 28.89% and 44.76%, respectively. The semiactive control performed best in terms of RMS transition, RMS speed and RMS acceleration, which were 22.77%, 48.33% and 52.10%, corresponding to 11.4% and 27.4% respectively: compared with the best passive case, it was lessened by 13.3%. Although the linear and quadratic regulator control effect is better, it can lessen by 1) 26.73%, 2) 56.39% and 3) 56.39%.

Fig. 7 reveals the status of the uncontrolled and controlled cables. Additionally, these curves clearly show that all passive, semiactive and linear and quadratic regulator controls have a significant control effect in reducing responses. As shown in the figure, semiactive control can be performed more effectively and efficiently and more passively than through effective control. Especially in moving from its place or position control, these performances of semiactive control is almost equal to that of linear and quadratic regulator control. In addition, it should be noted that semiactive control uses much fewer

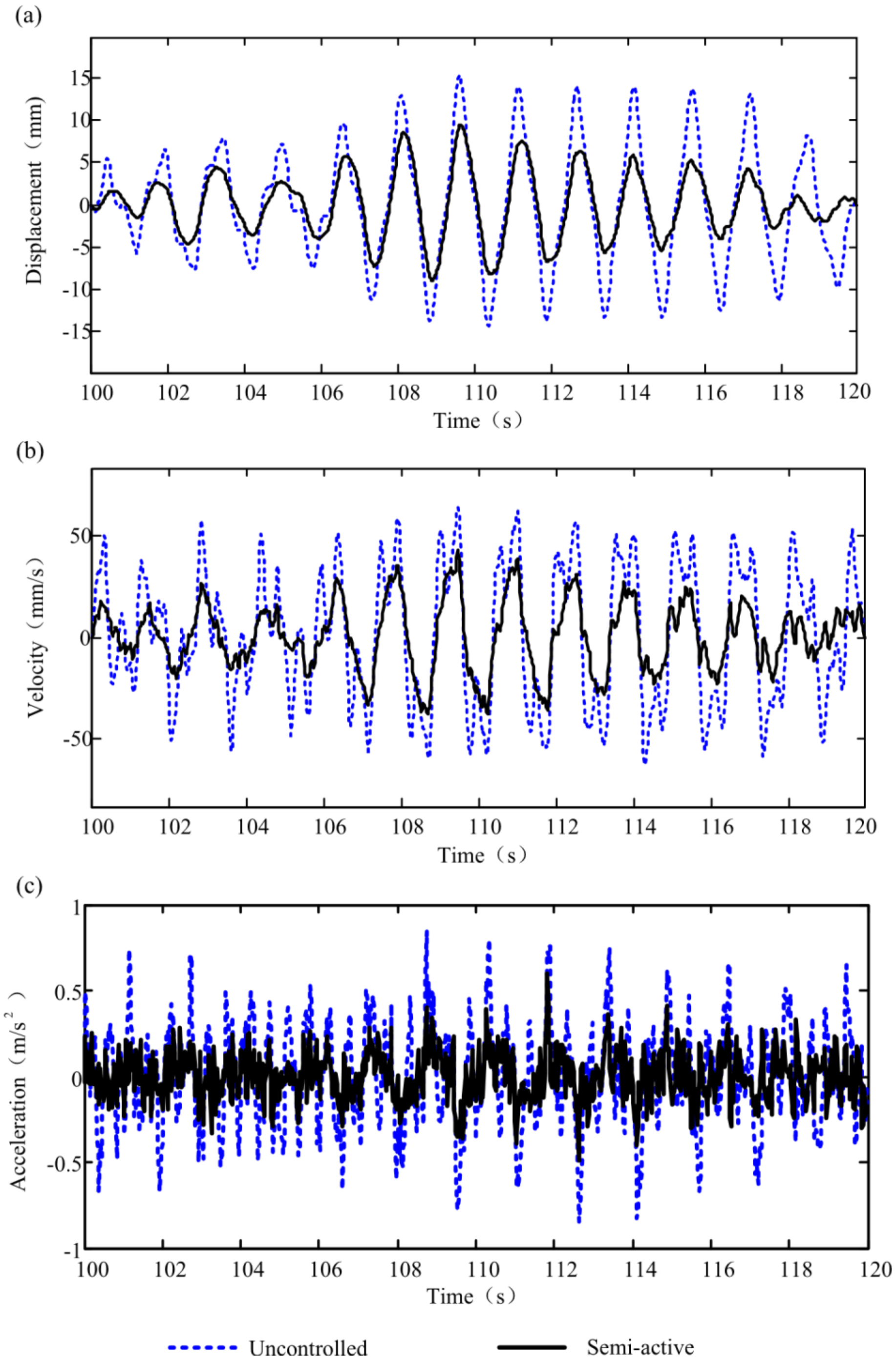

Fig.5 Comparison of tether vibrational response in uncontrolled and semiactive control, (a) the time history curve (b) the time history curve of speed (c) acceleration response

feedback points than linear and quadratic regulator control to achieve these performance levels. This is very important when using magnetic control image absorbers in actual designs.

Fig. 8 shows the MR damper can be seen that the semiactive regulator has obvious and negative stiffness characteristics, which can effectively and efficiently dissipate the vibrational energy of the cable. Therefore, using this evolutionary control numerical algorithm can effectively and efficiently alleviate the moving from its place or position and acceleration of the cable by using some fine-tuning sensors.

This paper investigates the performance of a semiactive control power system according to the newly put forward magnetic control resonance attenuator and the corresponding optimal control numerical algorithm. The design and manufacture of a single MR attenuator with the novel type of compensator aims to test its mechanical performance. By paying attention to the optimal linear and quadratic regulator control numerical algorithm, the corresponding optimal control numerical algorithm is present proposed. An important and interesting feature of

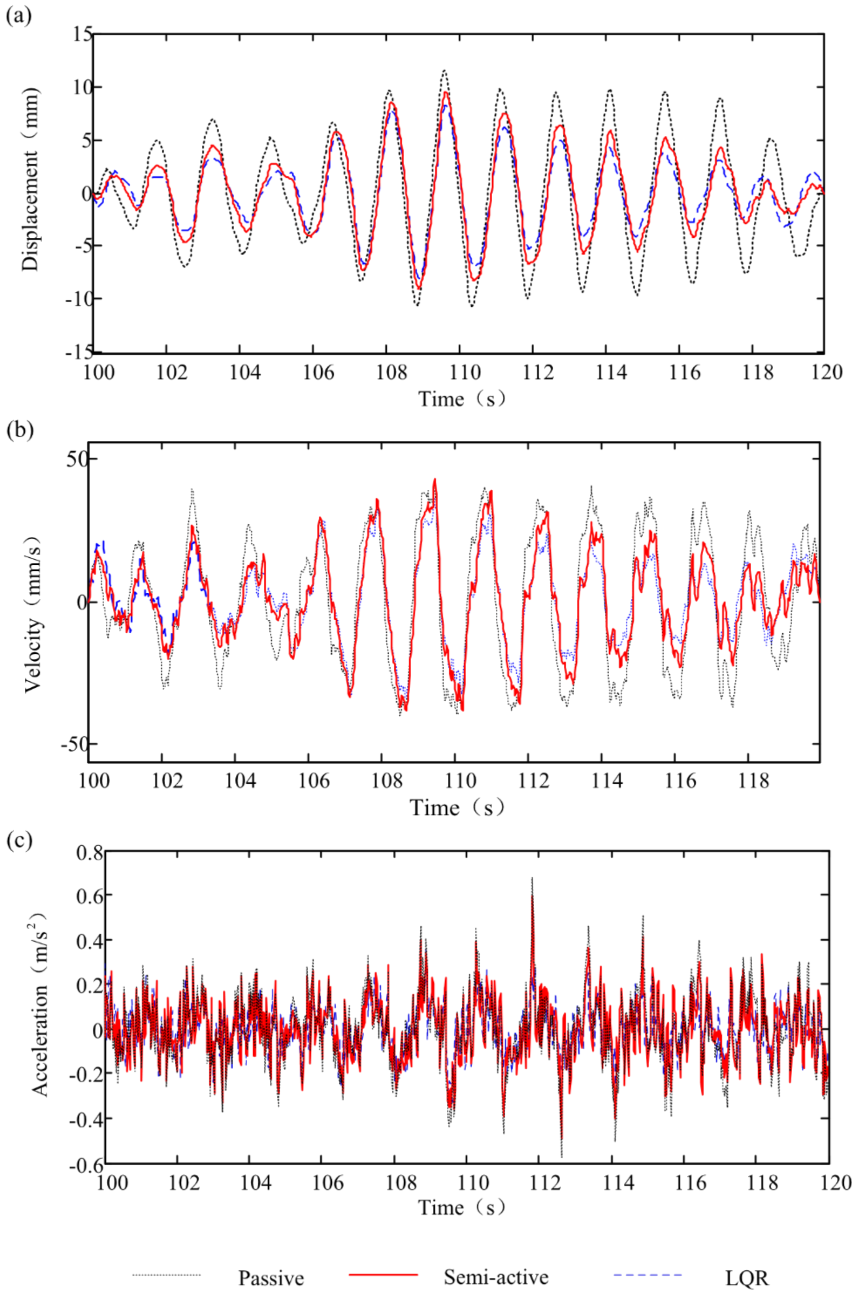

Fig. 6 Compare with the vibrational response with passive, semiactive and linear and quadratic regulator control, (a) the historical time curve, (b) velocity response, and (c) acceleration response

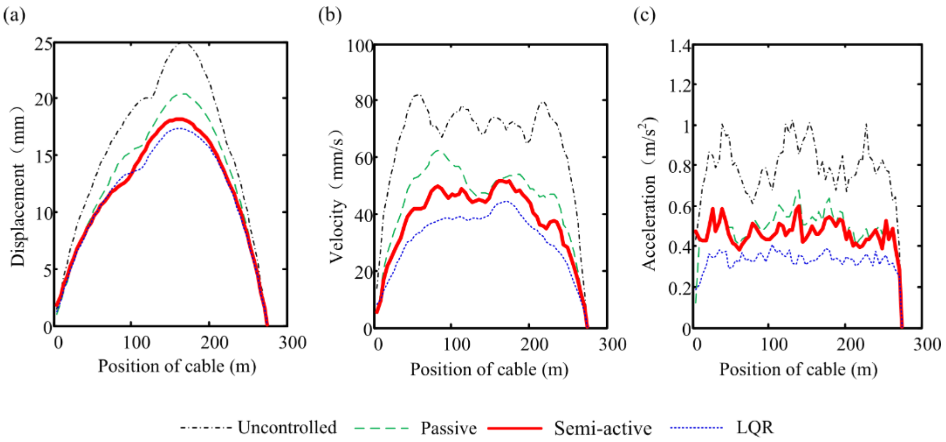

Fig. 7 The profiles of output for the stay cable

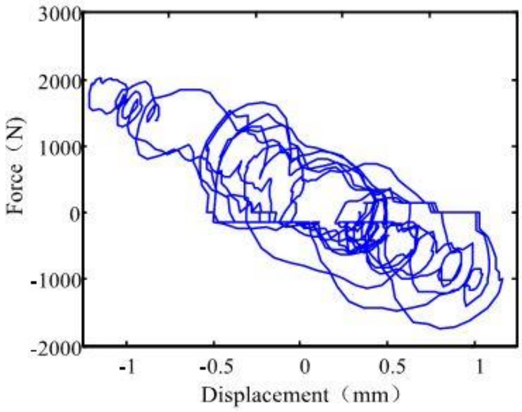

Fig. 8 The plot for the force (N) v.s. moving from its place or position (mm) by MR damper

the control numerical algorithm is that the optimal control force is significantly lessened, so it can be relatively realized. When comparing the best passive fuzzy control and linear and quadratic regulator control, this best equivalent control numerical algorithm was exploited to numerically evaluate the effectiveness of the MR attenuator, and the results were excellent. According to these results, we can have the findings that the newly put forward compensation design with respect to inner spring can understand the volume change requirements of the MR absorber and consider these directions of the damping-reduced force to optimize the optimal corresponding control numerical algorithm, and use the stay cable real-time feedback control and calculation.

6. Conclusions

This article discusses the issue of optimizing controller design issues, in which the evolutionary bat optimization numerical algorithm is combined with the fuzzy system controller in the practical application of the building. The controller of the system design includes different sub-parts such as system initial condition parameters, EB optimal numerical algorithm, fuzzy system controller, stability analysis and sensor actuator. The advantage of the design is that if the controller is useless, the modified criterion of controller is derived by asymptotically adjusting design parameters. Numerical verification of the time domain and the frequency domain shows that the new system design provides accurate prediction and control of the structural moving from its place or position response, which is necessary for the active control structure in the fuzzy numerical model. The dynamic fuzzy system controller present proposed in this present paper is exploited to find the optimal control force required for active nonlinear control of building structures.

References

Akgöz, B. and Civalek, Ö. (2013), “Buckling analysis of linearly tapered micro-columns based on strain gradient elasticity”, *Struct. Eng. Mech.*, **48**(2), 195-205. https://doi.org/10.12989/sem.2013.48.2.195.

Bhattacharyya, B. and Dalui, S.K. (2018), “Investigation of mean wind pressures on ‘E’plan shaped tall building”, *Wind Struct.*, **26**(2), 99-114. https://doi.org/10.12989/was.2018.26.2.099.

Chakraborty, S., Dalui, S.K. and Ahuja, A.K. (2014), “Wind load on irregular plan shaped tall building-a case study”, *Wind Struct.*, **19**(1), 59-73. https://doi.org/10.12989/was.2014.19.1.059.

Chen, C.W. (2014a), “Interconnected TS fuzzy technique for nonlinear time-delay structural systems”, *Nonlinear Dyn.*, **76**(1), 13-22. https://doi.org/10.1007/s11071-013-0841-8.

Chen, C.W. (2014b), “A criterion of robustness intelligent nonlinear control for multiple time-delay systems based on fuzzy Lyapunov methods”, *Nonlinear Dyn.*, **76**(1), 23-31. https://doi.org/10.1007/s11071-013-0869-9.

Chen, J. (2020), “System simulation and synchronization for optimal evolutionary design of nonlinear controlled systems”, *Smart Struct. Syst.*, **26**(6),797-807. http://dx.doi.org/10.12989/sss.2020.26.6.797.

Chen, L., Sun, L. and Nagarajaiah, S. (2016), “Cable vibration control with both lateral and rotational dampers attached at an intermediate location”, *J. Sound Vib.*, **377**, 38-57. https://doi.org/10.1016/j.jsv.2016.04.028.

Chen, T. (2020), “An intelligent algorithm optimum for building design of fuzzy structures”, *Iran J. Sci. Technol, Trans Civ. Eng.*, **44**, 523-531. https://doi.org/10.1007/s40996-019-00251-5.

Chen, T. (2020), “Evolved fuzzy NN control for discrete-time nonlinear systems”, *J. Circuits Syst. Comput.*, **29**(1), 2050015. https://doi.org/10.1142/S0218126620500152.

Chen, T. (2020), “On the algorithmic stability of optimal control with derivative operators”, *Circuits Syst. Signal Process*. https://doi.org/10.1007/s00034-020-01447-1.

Chen, T. (2021), “Optimized AI controller for reinforced concrete frame structures under earthquake excitation”, *Advan. Concrete Construct.*, **11**(1), https://doi.org/10.12989/acc.2021.11.1.000.

Chen, Z.H., Lam, K.H. and Ni, Y.Q. (2016), “Enhanced damping for bridge cables using a self-sensing MR damper”, *Smart Mater. Struct.*, **25**(8), 085019.

Chen, Z.Q., Wang, X.Y., Ko, J.M., Ni, Y.Q., Spencer, B.F., Yang, G. and Hu, J.H. (2004), “MR damping system for mitigating wind-rain induced vibration on Dongting Lake Cable-Stayed Bridge”, *Wind Struct.*, 7(5), 293-304.

Connor, J.J. (2003), *Introduction to Structural Motion Control*, Prentice-Hall: Upper Saddle River, N.J.

Dagnew, A. and Bitsuamlak, G.T. (2013), “Computational evaluation of wind loads on buildings: a review”, *Wind Struct.*, **16**(6), 629-660. http://dx.doi.org/10.12989/was.2013.16.6.629.

Djebien, R., Hebhoub, H., Belachia, M., Berdoudi, S. and Kherraf, L. (2018), “Incorporation of marble waste as sand in formulation of self-compacting concrete”, *Struct. Eng. Mech.*, **67**(1), 87-91. https://doi.org/10.12989/sem.2018.67.1.087.

Enns, D.F. (1984), “Model reduction with balanced realizations: An error bound and frequency weighted generalization”, *Proc. 23rd Conference on Decision and Control*, Las Vegas.

Gauthier, D.J., Sukow, D.W., Concannon, H.M. and Socolar, J.E. (1994), “Stabilizing unstable periodic orbits in a fast diode resonator using continuous time-delay autosynchronization”, *Phys. Rev. E.*, **50**(3), 2343. https://doi.org/10.1103/PhysRevE.50.2343.

Goksu, C., Saribas, I., Binbir, E., Akkaya, Y. and Ilki, A. (2019), “Structural performance of recycled aggregates concrete sourced from low strength concrete”, *Struct. Eng. Mech.*, **69**(1), 77-93. https://doi.org/10.12989/sem.2019.69.1.077.

Kalman, R.E. (1963), “New methods in Wiener filtering theory. In J.L. Bogdanoff and F. Kozin”, *Proceedings of the First Symposium on Engineering Applications of Random Function*

Theory and Probability. New York.
Maciejowski, J.M. (1989), *Multivariable Feedback Design*, Addition-Wesley Publishing Co., 222-264.
Mukherjee, S., Chakraborty, S., Dalui, S.K. and Ahuja, A.K. (2014), "Wind induced pressure on 'Y' plan shape tall building", *Wind Struct*., **19**(5), 523-540.
Muthuraj, H., Sekar, S.K., Mahendran, M., and Deepak, O.P. (2017), "Post buckling mechanics and strength of cold-formed steel columns exhibiting Local-Distortional interaction mode failure", *Struct. Eng. Mech*., **64**(5), 621-640.https://doi.org/10.12989/sem.2017.64.5.621.
Orod, Z. and Hamid Reza, K. (2016), "Experimental investigation on self-compacting concrete reinforced with steel fibers", *Struct. Eng. Mech*., **59**(1), 133-151.https://doi.org/10.12989/sem.2016.59.1.133.
Pinelli, J.P., Subramanian, C.S., Lapilli, C. and Buist, L. (2005), "Application of a wireless pressure sensing system to coastal wind monitoring", *Wind Struct*., **8**(3), 179-196.
Qissab, M.A. and Salman, M.M. (2018), "Shear strength of nonprismatic steel fiber reinforced concrete beams without stirrups", *Struct. Eng. Mech*., **67**(4), 347-358. https://doi.org/10.12989/sem.2018.67.4.347.
Tsai, P.W., Pan, J.S., Liao, B.Y., Tsai, M.J. and Istanda, V. (2012), "Bat algorithm inspired algorithm for solving numerical optimization problems", *Appl. Mech. Mater*., **148**, 134-137.
Wang, H.O. and Abed, E.H. (1995), "Bifurcation control of a chaotic system", *Automatica*, **31**(9), 1213-1226. https://doi.org/10.1016/0005-1098(94)00146-A.
Wang, H.O., Tanaka, K. and Griffin, M.F. (1996), "An approach to fuzzy control of nonlinear systems: Stability and design issues", *IEEE Transactions Fuzzy Syst*., **4**(1), 14-23. https://doi.org/10.1109/91.481841.
Xu, Z.D., Xu, M. and Sun, C.L. (2018), "Performance tests and microchain model validation of a novel kind of MR fluid with GO-coated iron particles", *J. Mater. Civil Eng*., **30**(5), 04018072. https://doi.org/10.1061/(ASCE)MT.1943-5533.0002253.

AD